The EMBO Journal Vol.18 No.5 pp.1114–1123, 1999

Structure of DNA-dependent protein kinase: implications for its regulation by DNA

Kerstin K.Leuther[1,2], Ola Hammarsten[3], Roger D.Kornberg[1] and Gilbert Chu[3,4]

[1]Department of Structural Biology and [3]Departments of Biochemistry and Medicine, Stanford University School of Medicine, Stanford, CA 94305, USA

[2]Present address: Affymax Research Institute, 4001 Miranda Avenue, Palo Alto, CA 94304, USA

[4]Corresponding author
e-mail: chu@cmgm.stanford.edu

K.K.Leuther and O.Hammarsten contributed equally to this work

DNA double-strand breaks are created by ionizing radiation or during V(D)J recombination, the process that generates immunological diversity. Breaks are repaired by an end-joining reaction that requires DNA-PK_{CS}, the catalytic subunit of DNA-dependent protein kinase. DNA-PK_{CS} is a 460 kDa serine-threonine kinase that is activated by direct interaction with DNA. Here we report its structure at 22 Å resolution, as determined by electron crystallography. The structure contains an open channel, similar to those seen in other double-stranded DNA-binding proteins, and an enclosed cavity with three openings large enough to accommodate single-stranded DNA, with one opening adjacent to the open channel. Based on these structural features, we performed biochemical experiments to examine the interactions of DNA-PK_{CS} with different DNA molecules. Efficient kinase activation required DNA longer than 12 bp, the minimal length of the open channel. Competition experiments demonstrated that DNA-PK_{CS} binds to double- and single-stranded DNA via separate but interacting sites. Addition of unpaired single strands to a double-stranded DNA fragment stimulated kinase activation. These results suggest that activation of the kinase involves interactions with both double- and single-stranded DNA, as suggested by the structure. A model for how the kinase is regulated by DNA is described.

Keywords: DNA-dependent protein kinase/DNA repair/electron crystallography/ionizing radiation/V(D)J recombination

Introduction

DNA double-strand breaks may be the most disruptive form of DNA damage. If left unrepaired, they lead to broken chromosomes and cell death. If repaired improperly, they can lead to chromosome translocations and cancer. In mammalian cells, double-strand breaks may be created in many ways, for example by exogenous agents such as ionizing radiation or endogenous processes such as V(D)J recombination, which is the site-specific recombination pathway that generates diversity in the immunoglobulin and T-cell receptor genes (Smider *et al*., 1994).

DNA-dependent protein kinase (DNA-PK) is a serine-threonine protein kinase that is activated by double-stranded DNA ends. At physiological salt concentrations, the enzyme requires two components to be active: a DNA-binding protein, Ku, and a catalytic subunit, DNA-PK_{CS} (Gottlieb and Jackson, 1993). Ku is a heterodimer of 70 and 86 kDa that binds to double-stranded DNA ends, nicks or transitions between double-stranded DNA and two single strands (Mimori and Hardin, 1986; Falzon *et al*., 1993). DNA-PK_{CS} is encoded by an open reading frame of 4096 amino acids, with a predicted mol. wt of 465.482 kDa (Hartley *et al*., 1995).

DNA-PK has generated considerable interest because it plays a key role in the repair of double-strand breaks created by ionizing radiation or V(D)J recombination (Smider *et al*., 1994; Taccioli *et al*., 1994; Blunt *et al*., 1995; Kirchgessner *et al*., 1995; Peterson *et al*., 1995). The severe combined immunodeficiency (scid) mouse (Bosma and Carroll, 1991) has a mutation in the DNA-PK_{CS} gene causing truncation of the terminal 83 amino acids in the kinase domain (Blunt *et al*., 1996; Danska *et al*., 1996), which leads to hypersensitivity to ionizing radiation (Fulop and Phillips, 1990; Biedermann *et al*., 1991) and a defect in V(D)J recombination characterized by undetectable coding joins in the face of relatively normal signal joins (Lieber *et al*., 1988). Mice generated by targeted disruption of the N-terminus (Gao *et al*., 1998) or C-terminal kinase domain of DNA-PK_{CS} (Taccioli *et al*., 1998) have a phenotype similar to that of the scid mouse, including a failure to make coding joins in the face of normal signal joins. These results provide genetic evidence for the importance of DNA-PK_{CS} in end-joining reactions during V(D)J recombination or following ionizing radiation.

DNA-PK_{CS} is a self-contained kinase that is activated by direct interaction with double-stranded DNA (Yaneva *et al*., 1997; Hammarsten and Chu, 1998). In low salt buffer, DNA-PK_{CS} is capable of binding to and activation by double-stranded DNA fragments, even in the absence of Ku. Binding of DNA-PK_{CS} to a double-stranded DNA fragment is disrupted by single-stranded poly(dT) or by circular double-stranded DNA (Hammarsten and Chu, 1998), properties distinct from the binding of Ku to DNA (Rathmell and Chu, 1994a,b). Furthermore, when the length of the DNA fragment decreased to 22 bp, Ku competed with DNA-PK_{CS} for DNA binding and inhibited kinase activity, demonstrating that DNA-PK_{CS} can be activated independently of Ku and that activation occurs by direct contact between DNA-PK_{CS} and DNA. Increasing salt to physiological concentrations inhibits the binding of DNA-PK_{CS} to DNA, so that efficient kinase activation

then requires the addition of Ku (Hammarsten and Chu, 1998). Thus, Ku has a role in stabilizing the binding of DNA-PK_{CS} to DNA ends. Recently, an end-joining reaction was reconstituted in a cell-free system (Baumann and West, 1998). The reaction involves DNA-PK_{CS} and is inhibited when the kinase is inhibited by wortmannin. Thus, the kinase activity of DNA-PK_{CS} appears to be required for the end-joining reaction in double-strand break repair.

Despite these advances, the biochemical role of DNA-PK in double-strand break repair and V(D)J recombination remains poorly defined. *In vivo* substrates for the kinase have not been identified, although Ku, DNA-PK_{CS} (Chan and Lees-Miller, 1996), XRCC4 (Leber *et al*., 1998) and the single-stranded DNA-binding protein RPA are candidates (Boubnov and Weaver, 1995; Fried *et al*., 1996). Apart from the kinase domain, the function of the remaining N-terminal 93% of the molecule has been hidden in the realm of speculation. The enormous size of DNA-PK_{CS} may allow it to act as a platform for mediating the synapsis of two DNA ends, processing the ends or recruiting other components to complete the end-joining reaction.

A complete understanding of the biochemical role of DNA-PK_{CS} will require detailed knowledge of its structure. The large size of the molecule is a daunting obstacle to solving the structure by X-ray crystallography. An alternative approach involves the formation of two-dimensional crystals on a lipid monolayer so that structural information can be obtained by electron microscopy (Kornberg and Darst, 1991; Jap *et al*., 1992; Brisson *et al*., 1994). This method has successfully elucidated structures of very large proteins and protein complexes. For example, structures were obtained for RNA polymerase II by itself (Darst *et al*., 1991) and in a complex with transcription factors TFIIB and TFIIE (Leuther *et al*., 1996).

Here we report the structure of DNA-PK_{CS} to a resolution of 22 Å. Among the features discerned in the structure are two open channels that potentially bind double-stranded DNA, and an enclosed cavity extending through the entire molecule that potentially binds single-stranded DNA. To relate the dimensions of this structure to its interaction with DNA, we measured activation and binding of the kinase with different DNA molecules. Efficient activation of the kinase required DNA longer than 12 bp, the minimal length of the open channels. Single-stranded DNA bound to DNA-PK_{CS} with kinetics suggesting a separate single-stranded DNA-binding site that interacts with the double-stranded DNA-binding site. These results are consistent with a role for the enclosed cavity in binding single-stranded DNA and regulating the kinase.

Results

Determination of the structure of DNA-PK_{CS} by electron crystallography

DNA-PK_{CS} was purified to virtual homogeneity and found to be capable of forming large two-dimensional crystals on a positively charged lipid layer. Negatively stained crystals diffracted to better than 20 Å resolution and were suitable for collection of tilt series and reconstruction of the three-dimensional structure of DNA-PK_{CS}. The three-dimensional structure was reconstructed from a total of 143 individual images.

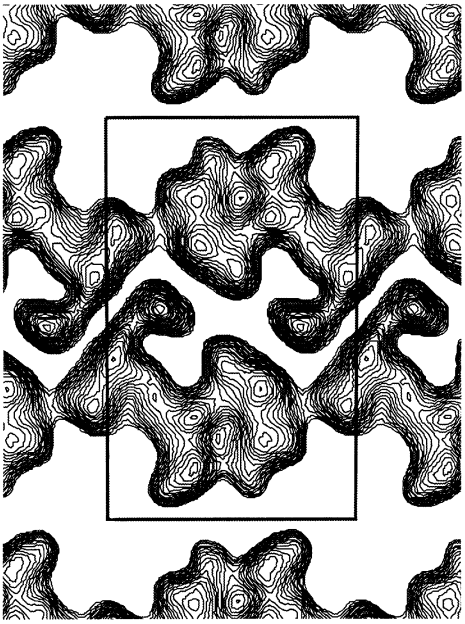

Fig. 1. Projection map of an untilted DNA-PK_{CS} crystal perpendicular to the plane of the lipid layer. The rectangle outlines one unit cell, which has dimensions $a = 150.3$ Å, $b = 234.6$ Å, and the angle between a and b, $\gamma = 89.6°$.

Table I. Quality and sampling for the three-dimensional data set in resolution bands

Resolution to (Å):	40	35	30	25	22	Overall
Percent sampling	83%	78%	81%	73%	49%	73%
Phase error	23°	31°	29°	31°	35°	30°
Multiplicity	24	17	14	10	8	15

Calculation of these numbers assumed data sampling to a 50° tilt, i.e. a 40° missing cone. Percent sampling refers to the percentage of possible structure factors observed. Phase error (°) is the average phase difference between measurements within 1/4T in z^*, where T is an estimate of the thickness of the molecule (here T = 100 Å) in the direction perpendicular to the plane of the crystal (z^* in reciprocal space). Multiplicity is a measurement of redundancy and refers to the average number of measurements recorded within half the sampling interval (0.0016/Å) from each sampled structure factor.

The projection map of an untilted image from a single DNA-PK_{CS} crystal is shown in Figure 1. Examination of several different crystals revealed two distinct classes, each class presenting a different surface of the DNA-PK_{CS} molecule. Two three-dimensional structures for DNA-PK_{CS} were reconstructed from the two classes, and the two structures were identical to each other, except for a rotation of 180° in the plane of the lipid. The concordance between the two structures provided an internal control for the reliability of the data. The images of both classes were then merged to obtain the final three-dimensional map. As shown in Table I, data to a resolution of 22 Å were well sampled in all resolution ranges as measured by multiplicity and percent sampling, and merged with reliable phase errors (Amos *et al*., 1982; Glaeser and Downing, 1992; Jensen *et al*., 1998).

At the electron dose for these experiments (<10 electrons per $Å^2$), shrinkage of the specimen is expected to

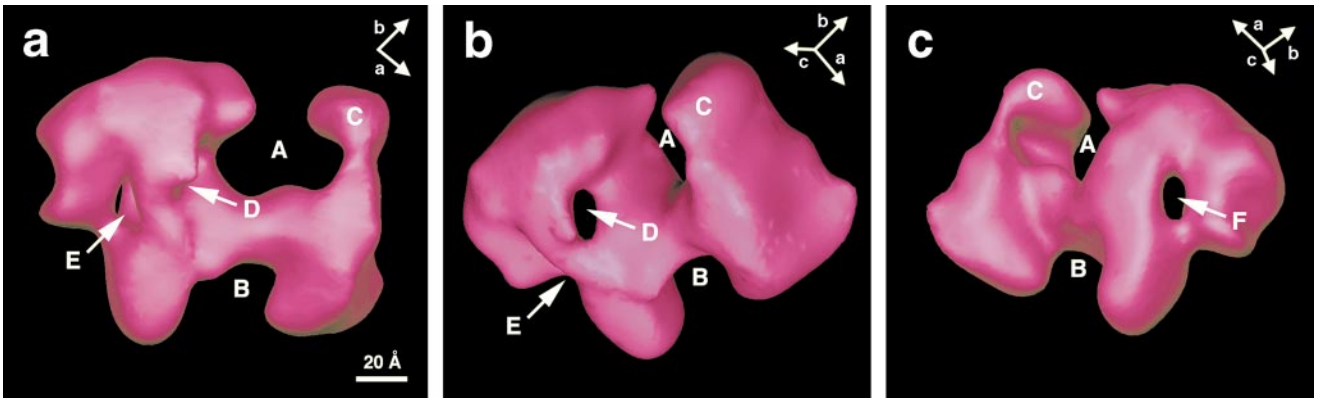

Fig. 2. Three-dimensional structure of the DNA-PK_{CS} molecule. (**a**) View perpendicular to the plane of the lipid layer. There are two open channels (labeled A and B) on opposite sides of the molecule. The feature labeled C indicates the protein density at the end of a potentially flexible arm that surrounds channel A. The arrows labeled D and E indicate two openings of an enclosed cavity. The arrows in the upper left corner of the figure indicate the direction of the unit cell axes *a* and *b*. The direction of axis *c* projects outward perpendicular to the *a*–*b* plane. (**b**) View showing the opening D of the enclosed cavity as it emerges adjacent to channel A. (**c**) View showing the other side of the molecule. Arrow F indicates a third opening of the enclosed cavity. Figures 2 and 3 were generated with the program SYNU (Hessler *et al*., 1992).

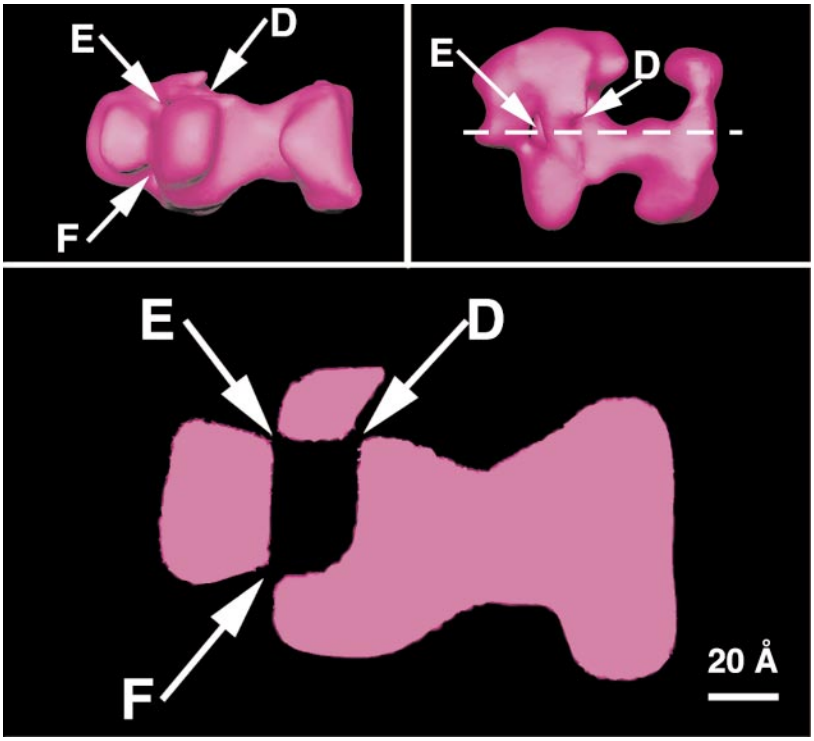

Fig. 3. Cross-sectional view of DNA-PK_{CS} showing the configuration of the enclosed cavity. The left inset shows the side view of the molecule looking into channel B, which results from rotation of the molecule in Figure 2A by 90° in the plane of the figure. The cross-sectional slice was taken close to the plane of this side view. The dashed line across the molecule in the right inset indicates the approximate location of the cross-sectional slice. The enclosed cavity has three separate openings. Since a single slice was chosen to pass through all three openings, none of the openings is shown in its widest dimension.

be minimal and should not affect the crystal structure within the resolution of the reconstruction. Sometimes the crystals folded over on the microscope grid, allowing us to verify that the unfolded crystal represented a single layer. Thus, the thickness of the crystal in the *z*-direction should be accurate to the stated resolution, although we do not have an independent direct measurement of thickness.

Figure 2 shows different views of the three-dimensional structure contoured at a level corresponding to 72% of the expected protein volume based on the molecular weight of DNA-PK_{CS} predicted from the amino acid sequence (465.482 kDa) (Hartley *et al*., 1995). This contour level is appropriate for specimens in negative stain (Amos *et al*., 1982; Darst *et al*., 1991; Jensen *et al*., 1998). When a control was performed with the contour level adjusted to 100% of the expected volume, the noise level in the structure remained very low, and all major structural features were preserved (including the features discussed below: three openings to an enclosed cavity and two open channels).

DNA-PK_{CS} is a relatively flat molecule with thickness varying from 39 to 75 Å (Figure 3), length measuring 135 Å in its longest dimension, and width varying from

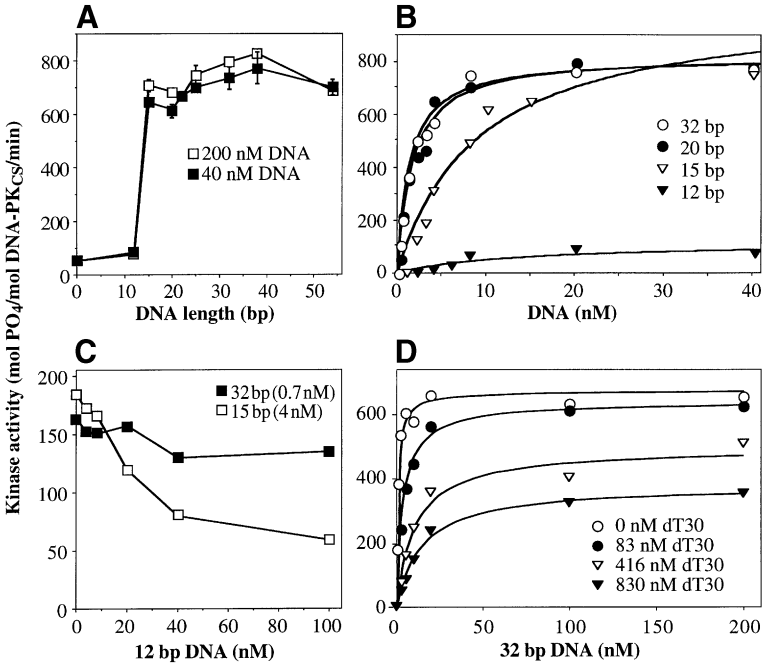

Fig. 4. Effects of DNA on DNA-PK_{CS} kinase activation. (**A**) Kinase activation as a function of DNA length. DNA 15, 20, 25, 32, 38 and 54 bp in length at saturating concentrations (40 and 200 nM) was incubated with DNA-PK_{CS} (7.6 nM). (**B**) Kinase activation as a function of DNA concentration. Different concentrations of DNA 12, 15, 20 and 32 bp in length were incubated with DNA-PK_{CS} (1.9 nM). (**C**) Kinase inhibition by 12 bp DNA. Different concentrations of 12 bp DNA together with subsaturating concentrations of 32 bp DNA (0.7 nM) or 15 bp DNA (4 nM) were incubated with DNA-PK_{CS} (1.9 nM). (**D**) Kinase inhibition by single-stranded DNA. Different concentrations of single-stranded DNA in the form of the 30 base oligonucleotide dT30 together with 32 bp DNA were incubated with DNA-PK_{CS} (1.9 nM).

107 to only 25 Å in the connecting protein density between two open channels (labeled A and B). Channel B is 31×19 Å and large enough to bind double-stranded DNA. Channel A, which is also large enough to bind double-stranded DNA, is significantly deeper than channel B, with an opening of 48×20 Å that is partially surrounded by an arm-like density. The protein density at the end of the arm-like feature (labeled C) is connected to the rest of the molecule by a hinge of low protein density, suggesting that the arm may be flexible. This structure bears some resemblance to the 'finger–palm–thumb' structure that forms the conserved catalytic center and nucleic acid-binding site in DNA and RNA polymerases (Darst *et al*., 1991; Joyce and Steitz, 1994; Sousa, 1996), although we found no significant sequence homology between DNA-PK_{CS} and the polymerases. Channel A is somewhat larger than that of the polymerases: the round cleft of DNA and RNA polymerases averages ~25 Å in diameter, while channel A is oblong and almost twice as wide (48×20 Å). However, its size might decrease significantly if the arm-like density (C) rotates around the hinge of low protein density when DNA occupies channel A.

Another conspicuous feature of DNA-PK_{CS} is an enclosed, oval cavity (8×16 Å) which extends through the entire molecule and is surrounded by protein density on all sides. Two openings (labeled D and E in Figure 2), separated by ~15 Å of protein density, allow access to the cavity from one side of the molecule, and an opening (labeled F) allows access from the other side. The complex geometry of the cavity is shown in Figure 3. Although the cavity is too small to accommodate double-stranded DNA, it is large enough for the threading of single-stranded DNA.

Effects of double- and single-stranded DNA on kinase activation

To gain insight into how the DNA interactions of DNA-PK_{CS} might reflect its structural features, we determined kinase activation as a function of DNA length for a series of double-stranded DNA molecules with blunt ends. First, DNA-PK_{CS} was incubated with a molar excess of DNA such that there was no significant change in kinase activity when DNA concentrations were increased from 40 to 200 nM (Figure 4A). Thus, the kinase activity in this experiment reflected DNA-PK_{CS} activity for saturating DNA concentrations (V_{max}). Significantly, V_{max} was low for a DNA length of 12 bp, but rose sharply to its maximal levels for a DNA length of 15 bp, remaining unchanged as DNA length increased up to 54 bp.

To investigate the threshold for kinase activation in greater detail, a range of lower DNA concentrations was used to test the activation of DNA-PK_{CS} (Figure 4B). The curves represent the best fits of the data to Michaelis–Menton kinetics. The V_{max} for kinase activation was very low for a DNA length of 12 bp and increased sharply to a constant value for DNA lengths of 15, 20 and 32 bp, confirming the result in Figure 4A. For 15 bp DNA, kinase activation reached half-saturating levels at a DNA concentration of 13 nM, so that K_m = 13 nM. This value was confirmed when it remained unaffected by a 4-fold increase in enzyme concentration to 7.6 nM (data not shown). For 20 and 32 bp DNA, kinase activation reached half-saturating levels at DNA concentrations of 1.6 and 1.3 nM, respectively, but these values increased when the enzyme concentration was increased. Lower enzyme concentrations would be required to determine accurately each K_m, but in our experiments this led to an unsatisfactory

loss of enzyme activity. Nevertheless, the data establish limits such that K_m <1.6 nM for 20 bp DNA, and K_m <1.3 nM for 32 bp DNA. These results suggest that the dissociation constant between DNA and the enzyme decreases as DNA length increases beyond 15 bp. This is consistent with a model in which the double-stranded DNA-binding site on DNA-PK_{CS} has the potential for sliding along the DNA, consistent with the structure of either open channel.

Although 12 bp DNA had a much lower V_{max} than longer DNA, its K_m was approximately the same as that for 15 bp DNA. This suggested that 12 bp DNA binds to the enzyme as effectively as 15 bp DNA. To demonstrate this directly, we tested whether 12 bp DNA was capable of inhibiting activation of DNA-PK_{CS} (Figure 4C). When the activating DNA was 32 bp DNA, the kinase was not significantly inhibited. In contrast, when the activating DNA was 15 bp DNA, the kinase was significantly inhibited at concentrations of 12 bp DNA near its K_m. As expected, inhibition was achieved down to the level of activation produced by 12 bp DNA alone. Thus, 12 bp DNA bound to DNA-PK_{CS} with about the same affinity as 15 bp DNA. However, efficient kinase activation was not achieved until DNA length was increased to 15 bp.

Because the enclosed cavity in DNA-PK_{CS} might represent a single-stranded DNA-binding site, we investigated the effect of single-stranded DNA on the kinase. The 30-base homopolymer dT30 by itself failed to activate the kinase (data not shown). Furthermore, dT30 inhibited activation of the kinase by 32 bp DNA (Figure 4D) or 15 bp DNA (data not shown). The dT30 produced a mixed inhibition, including a competitive component associated with an increase in K_m, and a non-competitive component associated with a decrease in V_{max} (Figure 4D).

Inhibition was specific for dT30 and not due to contaminants in the purified dT30 preparation, since complete reversal of inhibition occurred when dT30 was digested by S1 nuclease. This reversal occurred in the presence of the S1 digestion products of dT30, arguing against a non-specific effect of nucleotides on the ATP-binding site of the enzyme. Inhibition was unaffected by changes in peptide or ATP concentration, further evidence against non-specific effects on interaction of the enzyme with its peptide or ATP substrates. Inhibition was not peculiar to the homopolymer sequence, since a 32-base single-stranded oligonucleotide used to create the 32 bp DNA was also an effective inhibitor (data not shown). Thus, single-stranded DNA inhibited the kinase in a manner consistent with a direct interaction of single-stranded DNA with a binding site on DNA-PK_{CS}. The non-competitive component of the inhibition suggests that this binding site is distinct from the double-stranded DNA-binding site. The competitive component suggests an interaction between the double- and single-stranded DNA-binding sites, possibly reflecting the proximity of the enclosed cavity to channel A.

Since single-stranded DNA interacts with DNA-PK_{CS}, we wondered if double-stranded DNA activates DNA-PK_{CS} by binding in a configuration that includes single-stranded DNA. To test this possibility, we added five-base unpaired single-stranded ends to the 12 bp DNA fragment and measured its ability to activate the kinase. This structure activated the kinase 20-fold more efficiently than

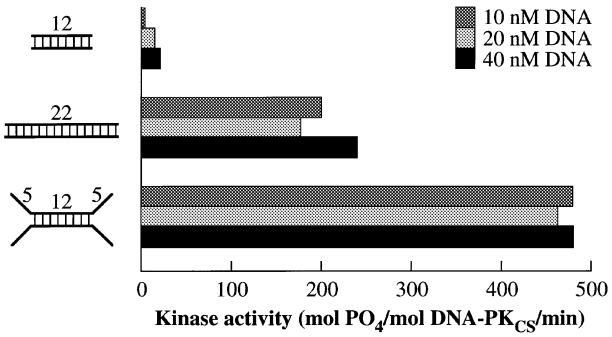

Fig. 5. DNA-PK_{CS} is activated most efficiently by a DNA fragment with unpaired single-stranded DNA ends. Activation of the kinase was measured using saturating concentrations of 12 bp double-stranded DNA, 22 bp double-stranded DNA or a DNA fragment containing 12 bp of double-stranded DNA with an additional five bases of unpaired single-stranded ends at each end.

the 12 bp double-stranded DNA fragment and 2-fold more efficiently than a 22 bp double-stranded DNA fragment (Figure 5). Thus, activation of DNA-PK_{CS} involves interactions with both double- and single-stranded DNA.

Binding of double- and single-stranded DNA to DNA-PK_{CS}

Our experiments suggested that DNA-PK_{CS} is capable of interacting with both double- and single-stranded DNA. To obtain direct evidence for such interactions, we explored different conditions in an electrophoretic mobility shift assay (EMSA). Best results were obtained when electrophoresis was performed in a relatively low salt buffer of 0.25× TGE (see Materials and methods). When purified DNA-PK_{CS} was incubated with the labeled single-stranded homopolymer dT30, we were able to detect a weak signal from protein–DNA complexes. When DNA-PK_{CS} was incubated with the longer single-stranded homopolymer dT54, the signal was significantly stronger, showing the formation of three distinct protein–DNA complexes. Two complexes migrated into the gel and a third complex was retained in the well of the gel (Figure 6A). The nature of these protein complexes remains to be defined, but a plausible hypothesis is that the fastest migrating complex contains a single DNA-PK_{CS} molecule and the slower migrating complex contains two DNA-PK_{CS} molecules. As expected, addition of unlabeled dT54 competitor DNA inhibited formation of the labeled complexes. Significantly, addition of unlabeled 32 bp double-stranded DNA also inhibited formation of the complexes, but less effectively than dT54. This result implies that DNA-PK_{CS} binds to double- and single-stranded DNA either at one binding site possessing a higher affinity for single-stranded DNA or at two separate sites that interact with each other.

To distinguish between these two possibilities, the reciprocal experiment was performed in which purified DNA-PK_{CS} was incubated with labeled 32 bp double-stranded DNA. The resulting protein–DNA complexes migrated at the same position as the complexes observed with labeled dT54 (Figure 6B). Addition of unlabeled 32 bp double-stranded DNA inhibited formation of the labeled complexes. However, addition of unlabeled single-stranded dT54 produced a small but reproducible increase in binding to the labeled 32 bp double-stranded DNA at low concentrations and a less pronounced inhibition than

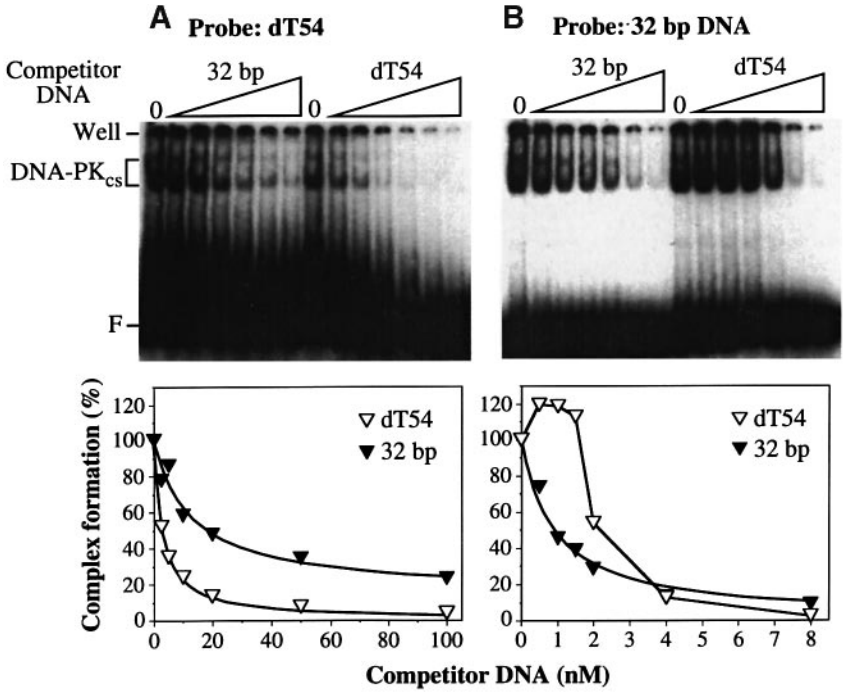

Fig. 6. DNA-PK_{CS} binds to single-stranded and double-stranded DNA at different sites. (**A**) Labeled single-stranded dT54 DNA probe was incubated with unlabeled double-stranded 32 bp DNA or unlabeled single-stranded dT54 DNA (2.5, 5, 10, 20, 50 and 100 nM) together with purified DNA-PK_{CS} in kinase buffer. (**B**) Labeled double-stranded 32 bp DNA probe was incubated with unlabeled double-stranded 32 bp DNA or unlabeled single-stranded dT54 DNA (0.5, 1, 1.5, 2, 4 and 8 nM) together with purified DNA-PK_{CS} in kinase buffer. For both DNA probes, the resulting protein–DNA complexes were analyzed by EMSA (top panels). The mobility shifts to the two DNA-PK_{CS} bands and to the well of the gel were quantified by phosphoimager to permit graphical representation of the binding activity (bottom panels).

with 32 bp DNA at higher concentrations. These results suggest that DNA-PK_{CS} contains two distinct but interacting binding sites for double- and single-stranded DNA. The results also raise the possibility that binding of single-stranded DNA to DNA-PK_{CS} can stimulate the binding of double-stranded DNA to the enzyme under some conditions, perhaps by inducing a conformational change in the structure.

Discussion

DNA-PK_{CS} contains interacting double- and single-stranded DNA-binding sites as suggested by its structure

The electron crystallographic structure provides a physical basis for the ability of double-stranded DNA to bind directly and activate DNA-PK_{CS}. The surface contour of DNA-PK_{CS} contains two open channels, each large enough to accommodate double-stranded DNA. Either open channel potentially explains the observations that DNA-PK_{CS} binds DNA at internal sites as well as DNA ends (Hammarsten and Chu, 1998).

The length of the channels spans the thickness of the DNA-PK_{CS} molecule, which varies from 39 to 75 Å, corresponding to DNA lengths of ~11–22 bp. These dimensions are consistent with the effect of DNA length on the biochemical properties of DNA-PK_{CS}. The maximum length of 75 Å provides a physical basis for the observation that 22 bp DNA will bind to and activate DNA-PK_{CS} but is too short to bind DNA-PK_{CS} and Ku simultaneously (Hammarsten and Chu, 1998). Conversely, the minimum length of 39 Å is consistent with our observation that although 12 bp DNA fails to activate the kinase efficiently, it is capable of binding to DNA-PK_{CS}.

The structure is also conspicuous for an enclosed cavity with three openings just large enough to accommodate single-stranded DNA. To test directly if DNA-PK_{CS} interacts with single-stranded DNA, we measured the effect of single-stranded DNA on kinase activation. Single-stranded DNA inhibited the activation of DNA-PK_{CS} by double-stranded DNA. The inhibition was mixed, with a non-competitive component suggesting a distinct binding site for single-stranded DNA. Using EMSA, we were able to demonstrate directly that DNA-PK_{CS} will bind to single-stranded DNA. DNA-PK_{CS} must have separate binding sites for double- and single-stranded DNA, since the single-stranded DNA-binding site had a lower affinity for double-stranded DNA, while the double-stranded DNA-binding site had a lower affinity for single-stranded DNA. Nevertheless, the two binding sites must interact with each other, since double-stranded DNA was able to inhibit binding of single-stranded DNA, and single-stranded DNA was able to inhibit binding of double-stranded DNA. We propose that the single-stranded DNA-binding site is the enclosed cavity.

Other proteins that interact with single-stranded DNA contain enclosed cavities. Lambda phage exonuclease is a homotrimeric protein surrounding a cavity large enough for double-stranded DNA at one end but just large enough for single-stranded DNA at the other end, consistent with its enzymatic activity (Kovall and Matthews, 1997). T5 phage 5′ exonuclease contains an enclosed arch defined by three α-helices, which are proposed to bind single-stranded DNA (Ceska *et al*., 1996). This arch is very

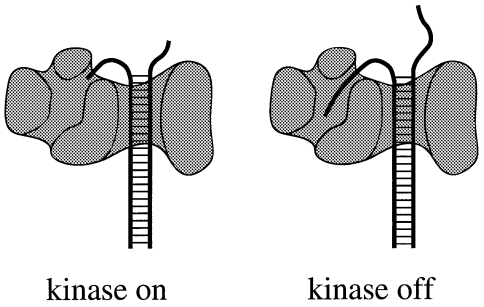

Fig. 7. Model for the interaction of DNA-PK_{CS} with single-stranded and double-stranded DNA. Double-stranded DNA binds to channel A in DNA-PK_{CS} and activates the kinase when a short single strand is threaded into the opening to the cavity adjacent to channel A. The activated kinase promotes processing of the DNA ends to generate longer unpaired single strands. When a single strand becomes long enough, it inhibits the kinase by penetrating deeply into the enclosed cavity either in the same molecule, as shown here, or in the DNA-PK_{CS} molecule bound to the opposing DNA end.

similar in size and shape to the enclosed cavity of DNA-PK_{CS}. The co-crystal of *Escherichia coli* Rep helicase and single-stranded DNA shows two conformations, one of which binds single-stranded DNA within a deep cleft, nearly surrounding the DNA with protein density (Korolev *et al*., 1997). Thus, when the structure of DNA-PK_{CS} is solved to atomic resolution, the cavity may prove to be either completely enclosed as seen for the lambda and T5 exonucleases, or potentially open as seen for Rep helicase.

Model for how DNA-PK_{CS} interacts with double- and single-stranded DNA

To explain the biochemical features of DNA-PK_{CS}, we propose a model in which the kinase is activated by a two-component interaction with DNA (Figure 7). The first component consists of the binding of double-stranded DNA to channel A, and the second component consists of the threading of one strand from the DNA end into the adjacent opening D to the enclosed cavity (Figures 2 and 3). Channel A (the proposed double-stranded DNA-binding site) has a minimal length of 39 Å, consistent with our finding that 12 bp DNA will bind to DNA-PK_{CS}. The distance from channel A to the adjacent cavity opening D (the proposed single-stranded DNA-binding site) is 20 Å, which is the length of 3–4 bases of unfolded single-stranded DNA (Bochkarev *et al*., 1997). Significantly, the addition of 3 bp of DNA to 12 bp DNA produces a large increase in the kinase V_{max} without significantly affecting binding affinity, consistent with one strand of the DNA just reaching the cavity opening D. The addition of five bases of unpaired single strands to each end of 12 bp DNA produces an even more substantial increase in V_{max}, consistent with threading of one of the single strands into the cavity opening D. This two-component interaction provides a structural basis for previous observations that circular DNA (Hammarsten and Chu, 1998) and DNA with covalently closed hairpin ends (Smider *et al*., 1998) bind to DNA-PK but fail to activate the kinase efficiently.

Although the dimensions of channels A and C are both appropriate for binding to double-stranded DNA, we favor channel A as the site that is coupled to kinase activation, given its proximity to the cavity opening D. It is possible that both channels serve as double-stranded DNA-binding sites. For example, one channel might bind one DNA end to activate the kinase, while the other channel binds to the opposing DNA end to facilitate synapsis of the two DNA ends.

In the context of our model, we also propose that the kinase is inhibited as single-stranded DNA penetrates more deeply into the cavity. This implies that the opening to the cavity adjacent to channel A participates in both activation and inhibition of the kinase. Thus, the single-stranded and double-stranded DNA-binding sites are distinct but interacting, consistent with our observation that dT30 acts as a mixed competitive and non-competitive inhibitor of the kinase.

The enclosed cavity has an opening E on the same face of the DNA-PK_{CS} molecule as opening D. This opening is located at a distance too great to be reached by five bases of unpaired DNA. However, it is possible that DNA-PK_{CS} facilitates synapsis of two DNA ends by dimerizing with itself, an event that may be represented by the slower migrating complex in Figure 6. In this context, when double-stranded DNA occupies channel A in one DNA-PK_{CS} molecule, one of the single-stranded ends is threaded into the adjacent opening D while the other single-stranded end is threaded into opening E in the second DNA-PK_{CS} molecule, aligning the two DNA molecules for the end-joining reaction.

One way in which DNA might activate DNA-PK_{CS} kinase activity is by inducing a conformational change to expose an active site on the enzyme. The model does not exclude the possibility that a similar conformational change might be induced in the absence of a DNA end. DNA-PK has been reported to be activated upon binding to negative regulatory element 1 from mouse mammary tumor virus (Giffin *et al*., 1997) or upon association with the high affinity DNA-binding protein C1D (Yavuzer *et al*., 1998). Thus, interaction either with a specific DNA sequence or with a particular protein may also promote a conformational change leading to kinase activation.

Role for DNA-PK_{CS} in DNA end-joining

The results reported here suggest a framework for understanding how DNA-PK_{CS} interacts with DNA to promote end-joining. When a DNA end is created either by ionizing radiation or by V(D)J recombination, Ku and DNA-PK_{CS} assemble at the end as the DNA-PK holoenzyme. At physiological salt concentration, Ku stabilizes the interaction between DNA-PK_{CS} and the DNA end, stimulating activation of the kinase (Hammarsten and Chu, 1998). Ku will bind to DNA structures either containing or potentially adopting a transition between double-stranded DNA and two single strands (Chu, 1997). We propose that Ku simulates the activation of DNA-PK_{CS} by utilizing the energy of DNA binding to separate the strands at the DNA end into an optimal conformation for kinase activation. To determine how Ku stimulates kinase activation, it will be important to crystallize Ku alone or in association with DNA or DNA-PK_{CS}. To test our hypotheses for the double- and single-stranded DNA-binding sites on DNA-PK_{CS}, it will be important to obtain co-crystals of DNA-PK_{CS} with DNA.

It is possible that the kinase activity of DNA-PK_{CS} is regulated during the DNA end-joining reaction to unwind the DNA ends further (Chu, 1997). This might occur

directly by insertion of a single strand into the enclosed cavity of DNA-PK_{CS} or indirectly by phosphorylation of Ku to activate a reported helicase activity (Tuteja *et al*., 1994). The kinase would be inactivated when a single strand becomes long enough to penetrate deeply into the enclosed cavity. It appears that end-joining is then completed when single strands from two opposing DNA ends are aligned by base pairing, unpaired DNA flaps are removed by a nuclease and the strands are joined covalently in a reaction involving XRCC4 protein and DNA ligase IV (Critchlow *et al*., 1997; Grawunder *et al*., 1997). The rejoined DNA thus contains a deletion limited by the extent of end unwinding. During V(D)J recombination, coding ends are joined with deletions <20 bp, consistent with alignment of single strands from opposing ends by pairing of one to five complementary bases from regions of microhomology. Regulation of DNA-PK_{CS} kinase activity by single-stranded DNA explains how a limitation is imposed on the extent of these deletions.

An understanding of the structure of DNA-PK_{CS} will have relevance for related proteins. DNA-PK_{CS} shares amino acid sequence homology with proteins in the phosphatidylinositol 3-kinase superfamily (Hartley *et al*., 1995), and aspects of its structure may be conserved among other members of the family, such as the ATM (Savitsky *et al*., 1995) and ATR (Zakian, 1995; Bentley *et al*., 1996; Cimprich *et al*., 1996) proteins, which also respond to DNA double-strand breaks.

Materials and methods

Electron crystallography

DNA-PK_{CS} was purified to 95% homogeneity as described previously (Hammarsten and Chu, 1998). For lipid layer crystallization, DNA-PK_{CS} was diluted into crystallization buffer [50 mM Tris pH 7.5, 20–25 mM NaCl and 10 mM dithiothreitol (DTT)] to a concentration of 90–100 μg/ml and pipeted into a cylindrical nylon well to form a flat surface. The aqueous surface was overlaid with a lipid mixture containing 0.45 mg/ml L-α-phosphatidylcholine and 0.05 mg/ml stearylamine (Avanti Polar Lipids) in 1:1 (v/v) chloroform/hexane. Samples were incubated for 12 h at 4°C in a water-saturated argon atmosphere. Crystals were transferred with Pt/Pd loops to glow-discharged carbon-coated electron microscope grids (Asturias and Kornberg, 1995). After washing with 0.05% Tween-20 and water, samples were stained for 35 s with 1% uranyl acetate.

Data collection and processing

All data were collected on a Phillips CM12 microscope in low dose mode (<10 electrons per $Å^2$) and operating at 100 kV with a LaB_6 filament. Images were recorded on Kodak SO136 film at a magnification of 35 000×. Up to seven exposures (the last one always untilted) could be taken from each crystal without significant loss of crystal quality. On average, four exposures were taken from each crystal. Quality of the micrographs was assessed by optical diffractometry, and suitable micrographs were scanned on a Leafscan 45 scanner with a 10 μm step size. Examination of the diffraction pattern of each crystal revealed two classes of crystals that were related by a 180° rotation. Initially, the two classes were processed separately, and resulted in two independently determined structures reconstructed from 61 (13 untilted, 48 tilted) and 82 (17 untilted, 65 tilted) images, respectively. Finally, the 30 untilted and 113 images tilted 14.6–60.1° to the incident electron beam were combined to yield the final three-dimensional map. All data processing was done with the MRC processing software (Amos *et al*., 1982; Henderson *et al*., 1986). Image processing was partially automated by programs obtained from G.Jensen (Jensen *et al*., 1998). All data were processed initially in the crystallographic plane group p1. Visual inspection of the resulting three-dimensional map, as well as evaluation of individual structure factor files with the program ALLSPACE (Valpuesta *et al*., 1994), confirmed that DNA-PK_{CS} crystallized in plane group p2 (unique axis *c*). This symmetry was then imposed throughout merging in ORIGTILT and throughout generation of amplitudes and phases representing structure factors from all data by the program LATLINE (Agard, 1983). The absolute handedness of the structure was determined as described (Amos *et al*., 1982), and was examined at several stages of the reconstruction. As detailed in Table I, 73% of possible structure factors were observed to 22 Å resolution with an overall phase error of 30° and a missing cone of 40°. Phase error statistics were calculated with a program by G.Jensen (Jensen *et al*., 1998), which was modified to accept p2 data. Maps were displayed with the program XtalView (McRee, 1992). One unit cell contains two molecules of DNA-PK_{CS} and has dimensions of a = 150.3 Å, b = 234.6 Å, γ = 89.6°.

Kinase assay

Purified DNA-PK_{CS} was activated by DNA in the presence of the specific peptide substrate EPPLSQEAFADLWKK (0.3 mM) and a saturating concentration of ATP (1.25 μCi [γ-^{32}P]ATP plus 0.06–0.25 mM unlabeled ATP) in a volume of 10 μl of kinase buffer (10 mM Tris–HCl pH 7.4, 1 mM EDTA, 10 mM mercaptoethanol, 20 mM $MgCl_2$, 5% glycerol). Phosphate transfer to the peptide was measured as described (Hammarsten and Chu, 1998) after 4–6 min at 37°C, during which phosphate transfer increased linearly with time. DNA molecules were derived from oligonucleotides of 12, 15, 20, 22, 25, 32, 38 and 54 bases, each purified on OPC columns (Poly-pak™ cartridge, Glen Research). The oligonucleotides were derived from the 54-base oligonucleotide (5′-GGCCGCACGCGTCCACCATGGGGTACAACTACGATCTAGCTT-CATGCACCGGAC-3′) with successive shortening from the 3′ end. Blunt-ended double-stranded DNA molecules were created by annealing complementary oligonucleotides in a 1:1 molar ratio. To remove contaminating single-stranded DNA, the annealed DNA was resolved in a 12% non-denaturing polyacrylamide gel and then stained with ethidium bromide. The double-stranded DNA band was excised, eluted by passive diffusion, extracted with butanol, phenol/chloroform and chloroform, and precipitated in ethanol. Further purification was achieved with the MERmaid kit (Bio101, Vista, CA) to remove non-nucleic acid contaminants that inhibited the kinase. To confirm the removal of single-stranded DNA, the preparations were labeled with polynucleotide kinase and analyzed by non-denaturing polyacrylamide gel electrophoresis. The DNA fragment with single-stranded ends was created by adding five bases of dT to the 3′ and 5′ ends of both strands of the 12 bp DNA fragment. The single-stranded oligonucleotide dT30 was purified on a Hypersil C18 HPLC column (Sigma), lyophilized, resuspended and dialyzed against buffer containing 10 mM Tris pH 8.0 and 1 mM EDTA.

Electrophoretic mobility shift assay

The DNA-binding activity of DNA-PK_{CS} was determined by EMSA by modification of a previously described procedure (Hammarsten and Chu, 1998). Labeled double-stranded 32 bp DNA (0.5 nM) or the single-stranded homopolymer dT54 (2.5 nM) was mixed with competitor DNA in 10 μl of kinase buffer supplemented with bovine serum albumin (0.5 mg/ml) and ATP (0.06 mM) before addition of DNA-PK_{CS} (10 nM). The mixture was incubated for 10 min at room temperature and then resolved by electrophoresis in a 4% polyacrylamide gel in 0.25× TGE buffer (1× TGE is 50 mM Tris pH 8.5, 0.38 M glycine, 2 mM EDTA). The single-stranded dT54 was purified on a DNAPAC HPLC column (Dynal), desalted on a SepPac column (Waters), lyophilized and resuspended in buffer containing 10 mM Tris pH 8.0 and 1 mM EDTA.

Acknowledgements

We thank Peter David and Grant Jensen for help with program modifications, Peter David and Richard Henderson for advice on space group determination, and Dan Herschlag, Claes and Maria Gustafsson, Suzanne Admiral, Lisa Defazio and Vaughn Smider for advice on the biochemistry. K.K.L. was supported by a postdoctoral fellowship from the American Cancer Society. O.H. was supported by the Swedish Cancer Society, STINT, Gothenburg Medical Society, King Gustav V Jubilee Clinic Cancer Research Foundation and Swedish Medical Society. The research was supported by gifts from Graham and Jane Nissen and grant DAMD 17-94-J-4350 from the US Army Medical Research and Materiel Command to G.C. and by NIH grant AI21144 to R.K.

References

Agard,D.A. (1983) A least squares method for determining structure factors in three-dimensional tilted-view reconstructions. *J. Mol. Biol*., **167**, 849–852.

Amos,L.A., Henderson,R. and Unwin,P.N. (1982) Three-dimensional structure determination by electron microscopy of two-dimensional crystals. *Prog. Biophys. Mol. Biol.*, **39**, 183–231.

Asturias,F.J. and Kornberg,R.D. (1995) A novel method for transfer of two-dimensional crystals from the air–water interface to specimen grids. *J. Struct. Biol.*, **114**, 60–66.

Baumann,P. and West,S.C. (1998) DNA end-joining catalyzed by human cell-free extracts. *Proc. Natl Acad. Sci. USA*, **95**, 14066–14070.

Bentley,N.J., Holtzman,D.A., Flaggs,G., Keegan,K.S., DeMaggio,A., Ford,J.C., Hoekstra,M. and Carr,A.M. (1996) The *S.pombe rad3* checkpoint gene. *EMBO J.*, **15**, 6641–6651.

Biedermann,K.A., Sun,J.R., Giaccia,A.J., Tosto,L.M. and Brown,J.M. (1991) Scid mutation in mice confers hypersensitivity to ionizing radiation and a deficiency in DNA double-strand break repair. *Proc. Natl Acad. Sci. USA*, **88**, 1394–1397.

Blunt,T. *et al*. (1995) Defective DNA-dependent protein kinase activity is linked to V(D)J recombination and DNA repair defects associated with the murine scid mutation. *Cell*, **80**, 813–823.

Blunt,T., Gell,D., Fox,M., Taccioli,G.E., Lehman,A.R., Jackson,S.P. and Jeggo,P.A. (1996) Identification of a nonsense mutation in the carboxy-terminal region of DNA-dependent protein kinase catalytic subunit in the scid mouse. *Proc. Natl Acad. Sci. USA*, **93**, 10285–10290.

Bochkarev,A., Pfuetzner,R.A., Edwards,A.M. and Frappier,L. (1997) Structure of the single-stranded DNA-binding domain of replication protein A bound to DNA. *Nature*, **385**, 176–181.

Bosma,M.J. and Carroll,A.M. (1991) The SCID mouse mutant: definition, characterization and potential uses. *Annu. Rev. Immunol.*, **9**, 323–350.

Boubnov,N.V. and Weaver,D.T. (1995) Scid cells are deficient in Ku and replication protein A phosphorylation by the DNA-dependent protein kinase. *Mol. Cell. Biol.*, **15**, 5700–5706.

Brisson,A., Olofsson,A., Ringler,P., Schumtz,M. and Stoylova,S. (1994) Two-dimensional crystallization of proteins on planar lipid films and structure determination by electron crystallography. *Cell*, **80**, 221–228.

Ceska,T.A., Sayers,J.R., Stier,G. and Suck,D. (1996) A helical arch allowing single-stranded DNA to thread through T5 5′-exonuclease. *Nature*, **382**, 90–93.

Chan,D.W. and Lees-Miller,S. (1996) The DNA-dependent protein kinase is inactivated by autophosphorylation of the catalytic subunit. *J. Biol. Chem.*, **271**, 8936–8941.

Chu,G. (1997) Double-strand break repair. *J. Biol. Chem.*, **272**, 24097–24100.

Cimprich,K.A., Shin,T.B., Keith,C.T. and Schreiber,S.L. (1996) cDNA cloning and gene mapping of a candidate human cell cycle checkpoint protein. *Proc. Natl Acad. Sci. USA*, **93**, 2850–2855.

Critchlow,S.E., Bowater,R.P. and Jackson,S.P. (1997) Mammalian DNA double-strand break repair protein XRCC4 interacts with DNA ligase IV. *Curr. Biol.*, **7**, 588–598.

Danska,J.S., Holland,D.P., Mariathasan,S., Williams,K.M. and Guidos,C.J. (1996) Biochemical and genetic defects in the DNA-dependent protein kinase in murine scid lymphocytes. *Mol. Cell. Biol.*, **16**, 5507–5517.

Darst,S.A., Edwards,A.M., Kubalek,E.W. and Kornberg,R.D. (1991) Three-dimensional structure of yeast RNA polymerase II at 16 Å resolution. *Cell*, **66**, 121–128.

Falzon,M., Fewell,J.W. and Kuff,E.L. (1993) EBP-80, a transcription factor closely resembling the human autoantigen Ku, recognizes single- to double-strand transitions in DNA. *J. Biol. Chem.*, **268**, 10546–10552.

Fried,L.M. *et al*. (1996) The DNA damage response in DNA-dependent protein kinase-deficient SCID mouse cells: replication protein A hyperphosphorylation and p53 induction. *Proc. Natl Acad. Sci. USA*, **93**, 13825–13830.

Fulop,G.M. and Phillips,R.A. (1990) The scid mutation in mice causes a general defect in DNA repair. *Nature*, **347**, 479–482.

Gao,Y., Chaudhuri,J., Zhu,C., Davidson,L., Weaver,D.T. and Alt,F.W. (1998) A targeted DNA-PKcs-null mutation reveals DNA-PK-independent functions for KU in V(D)J recombination. *Immunity*, **9**, 367–376.

Giffin,W., Kwast-Welfeld,J., Rodda,D.J., Prefontaine,G.G., Traykova-Andonova,M., Zhang,Y., Weigel,N.L., Lefebvre,Y.A. and Hache,R.J. (1997) Sequence-specific DNA binding and transcription factor phosphorylation by Ku autoantigen/DNA-dependent protein kinase. *J. Biol. Chem.*, **272**, 5647–5658.

Glaeser,R.M. and Downing,K.H. (1992) Assessment of resolution in biological electron crystallography. *Ultramicroscopy*, **47**, 256–265.

Gottlieb,T.M. and Jackson,S.P. (1993) The DNA-dependent protein kinase: requirement for DNA ends and association with Ku antigen. *Cell*, **72**, 131–142.

Grawunder,U., Wilm,M., Xiantuo,W., Kulezla,P., Wilson,T.E., Mann,M. and Lieber,M.R. (1997) Activity of DNA ligase IV stimulated by complex formation with XRCC4 protein in mammalian cells. *Nature*, **388**, 492–494.

Hammarsten,O. and Chu,G. (1998) DNA-dependent protein kinase: DNA binding and activation in the absence of Ku. *Proc. Natl Acad. Sci. USA*, **95**, 525–530.

Hartley,K.O. *et al*. (1995) DNA-dependent protein kinase catalytic subunit: a relative of phosphatidylinositol 3-kinase and the ataxia telangiectasia gene product. *Cell*, **82**, 849–856.

Henderson,R., Baldwin,J.M., Downing,K., Lepault,J. and Zemlin,F. (1986) Structure of purple membrane from *Halobacterium halobium*: recording, measurement and evaluation of electron micrographs at 3.5 Å resolution. *Ultramicroscopy*, **19**, 147–178.

Hessler,D. *et al*. (1992) Programs for visualization in three-dimensional microscopy. *Neuroimage*, **1**, 55–67.

Jap,B.K., Zulauf,M., Scheybani,T., Hefti,A., Baumeister,W., Aebi,U. and Engel,A. (1992) 2-D crystallization: from art to science. *Ultramicroscopy*, **46**, 45–84.

Jensen,G.J., Meredith,G., Bushnell,D.A. and Kornberg,R.D. (1998) Structure of wild type yeast RNA polymerase II and location of Rpb4 and Rpb7. *EMBO J.*, **17**, 2353–2358.

Joyce,C.M. and Steitz,T.A. (1994) Function and structure relationships in DNA polymerases. *Annu. Rev. Biochem.*, **63**, 777–822.

Kirchgessner,C., Patil,C., Evans,J., Cuomo,C., Fried,L., Carter,T., Oettinger,M. and Brown,J.M. (1995) DNA-dependent kinase (p350) as a candidate gene for the murine SCID defect. *Science*, **267**, 1178–1185.

Kornberg,R.D. and Darst,S.A. (1991) Two-dimensional crystals of proteins on lipid layers. *Curr. Opin. Struct. Biol.*, **1**, 642–646.

Korolev,S., Hsieh,J., Gauss,G., Lohman,T. and Waksman,G. (1997) Major domain swiveling revealed by the crystal structures of complexes of *E.coli* Rep helicase bound to single-stranded DNA and ADP. *Cell*, **90**, 635–647.

Kovall,R. and Matthews,B. (1997) Toroidal structure of λ-exonuclease. *Science*, **277**, 1824–1827.

Leber,R., Wise,T., Mizuta,R. and Meek,K. (1998) The *XRCC4* gene product is a target for and interacts with the DNA-dependent protein kinase. *J. Biol. Chem.*, **273**, 1794–1801.

Leuther,K.K., Bushnell,D.A. and Kornberg,R.D. (1996) Two-dimensional crystallography of TFIIB- and IIE-RNA polymerase II complexes: implications for start site selection and initiation complex formation. *Cell*, **85**, 773–779.

Lieber,M.R., Hesse,J.E., Lewis,S., Bosma,G.C., Rosenberg,N., Mizuuchi,K., Bosma,M.J. and Gellert,M. (1988) The defect in murine severe combined immune deficiency: joining of signal sequences but not coding segments in V(D)J recombination. *Cell*, **55**, 7–16.

McCree,D.E. (1992) A visual protein crystallographic software system for XII/X view. *J. Mol. Graph.*, **10**, 44–46.

Mimori,T. and Hardin,J.A. (1986) Mechanism of interaction between Ku protein and DNA. *J. Biol. Chem.*, **261**, 10375–10379.

Peterson,S.R., Kurimasa,A., Oshimura,M., Dynan,W.S., Bradbury,E.M. and Chen,D.J. (1995) Loss of the catalytic subunit of the DNA-dependent protein kinase in DNA double-strand-break-repair mutant mammalian cells. *Proc. Natl Acad. Sci. USA*, **92**, 3171–3174.

Rathmell,W.K. and Chu,G. (1994a) A DNA end-binding factor involved in double-strand break repair and V(D)J recombination. *Mol. Cell. Biol.*, **14**, 4741–4748.

Rathmell,W.K. and Chu,G. (1994b) Involvement of the Ku autoantigen in the cellular response to DNA double-strand breaks. *Proc. Natl Acad. Sci. USA*, **91**, 7623–7627.

Savitsky,K. *et al*. (1995) A single ataxia-telangiectasia gene with product similar to PI-3 kinase. *Science*, **268**, 1749–1753.

Smider,V., Rathmell,W.K., Lieber,M. and Chu,G. (1994) Restoration of X-ray resistance and V(D)J recombination in mutant cells by Ku cDNA. *Science*, **266**, 288–291.

Smider,V., Rathmell,W.K., Brown,G., Lewis,S. and Chu,G. (1998) Failure of hairpin-ended and nicked DNA to activate DNA-dependent protein kinase: implications for V(D)J-recombination. *Mol. Cell. Biol.*, **18**, 6853–6858.

Sousa,R. (1996) Structural and mechanistic relationships between nucleic acid polymerases. *Trends Biochem. Sci.*, **21**, 186–190.

Taccioli,G.E. *et al*. (1994) Ku80: product of the *XRCC5* gene and its role in DNA repair and V(D)J recombination. *Science*, **265**, 1442–1445.

Taccioli,G.E. *et al*. (1998) Targeted disruption of the catalytic subunit of the DNA-PK gene in mice confers severe combined immunodeficiency and radiosensitivity. *Immunity*, **9**, 355–366.
Tuteja,N. *et al*. (1994) Human DNA helicase II: a novel DNA unwinding enzyme identified as the Ku autoantigen. *EMBO J.*, **13**, 4991–5001.
Valpuesta,J.M., Carrascosa,J.L. and Henderson,R. (1994) Analysis of electron microscope images and electron diffraction patterns of thin crystals of Ø29 connectors in ice. *J. Mol. Biol.*, **240**, 281–287.
Yaneva,M., Kowalewski,T. and Lieber,M. (1997) Interaction of DNA-dependent protein kinase with DNA and with Ku: biochemical and atomic-force microscopy studies. *EMBO J.*, **16**, 5098–5112.
Yavuzer,U., Smith,G.C., Bliss,T., Werner,D. and Jackson,S.P. (1998) DNA end-independent activation of DNA-PK mediated via association with the DNA-binding protein C1D. *Genes Dev.*, **12**, 2188–2199.
Zakian,V.A. (1995) ATM-related genes: what do they tell us about functions of the human gene? *Cell*, **82**, 685–687.

Received September 18, 1998; revised and accepted January 5, 1999